Real-time structural health monitoring of reinforced concrete frame structure using a hysteresis loop method

2015 NZSEE Conference

C. Zhou, J.G. Chase & G.W. Rodgers

Department of Mechanical Engineering, University of Canterbury, Christchurch

C. Xu

School of Astronautics, Northwestern Polytechnical University, Xi'an, China

ABSTRACT: This research investigates a rapid structural health monitoring method for civil structures that delivers results immediately after a major seismic event. The method is based on an overall least squares regression analysis and hypothesis test, and is applied to an experimental scaled 12-story reinforced concrete frame structure subjected to two stages of input ground motions. The test structure is simplified to a six degree of freedom (DOF) system model, where the accelerations of each DOF are recorded. Nonlinear hysteresis loops are reconstructed for each DOF, and divided into a number of half cycles in chronological order. Changes in identified elastic story stiffness in these selected half cycles are used as an index for damage localization and severity assessment, and tracked over time using the proposed identification algorithm.

The feasibility and robustness of the proposed monitoring algorithm is validated using the data from the experimental test structure. No large drop of elastic stiffness was identified for the test structure under the small input ground motion. Significant stiffness degradation was identified for the fourth, third and second DOF with stiffness losses over 50% compared to the calculated initial stiffness. Cracks were also observed at the beam-column joint connection at floors six, five and four after the experiment for the strong input ground motion. The results indicate the identification algorithm is capable of detection and assessing the damage location and severity automatically by tracking the evolution of elastic story stiffness without requiring human input.

1 INTRODUCTION

Recently, real-time data acquisition from the instrumented structure has become a more feasible reality with the significant development of sensors, such as fibre optic sensors (Ko and Ni 2005), wireless sensors (Spencer et al. 2004), piezoelectric sensors (Baptista et al. 2012) and force-balanced accelerometers that are specially designed for installation in civil engineering for commercial monitoring systems (Hsieh et al. 2006). Based on these newer sensor technologies, the recorded response data can then transmitted over the internet to the identification algorithm to detect and localize the seismic damage by considering the changes of one or more damage indices during or soon after an earthquake event. Equally, computation could be done locally if required in real-time.

Many damage detection algorithms are vibration-based SHM methods that identify changes in conventional linear damage indices, including natural frequency, mode shapes and modal damping, due to changes in stiffness, damping and/or physical mass (Doebling et al. 1996). However, these methods might not be sufficient to localize or assess the severity of damage in some cases. In particular, damage in two different locations of a larger or more complex structure could lead to the same changes in those conventional damage indices (Vafaei et al. 2013). Further, these methods are more applicable to structures where vibration response is high linear (Chase et al. 2005a), which implies minimal damage and thus a lesser need for monitoring.

Monitoring elastic and/or plastic stiffness, as well as plastic deformation have also been employed for damage detection in many other methods, such as least squares estimation (LSE) (Smyth et al. 2002; Yang and Lin 2004) and adaptive least mean squares (LMS) (Chase et al. 2005a; Chase et al. 2005b) methods. These methods can be used to track the changes of stiffness that reflect structural behaviour due to damage. However, both the LSE and LMS algorithms require a full state of structural response measurements, which is not typically and easily available. A modified LMS method can be used to identify both changes in stiffness and plastic deformation, but only with high sampling rate acceleration and low-frequency sampled displacement (Nayyerloo et al. 2011). However, they are not as effective for nonlinear yielding structures, especially with complex hysteretic behaviour, such as pinching. The extended Kalman filter (EKF) algorithm is one of the widely used algorithms for nonlinear structure, and it only requires the recorded acceleration response (Loh et al. 2000; Wu and Smyth 2008). However, for highly nonlinear structure, the accuracy and convergence of the estimation depend on the quality of the initial guesses of unknown parameters. It is also sensitive to the addition of noise in the measured response. Thus, there are still significant limitations in all these methods, which limit realistic nonlinear monitoring.

In addition, many current SHM algorithms are based on a proposed baseline model. These model-based method can perform effectively when the numerical model is suitable to represent the real system. However, they can produce erratic results when the model is not well defined (Yao and Pakzad 2014). Hence, if a good baseline model is not available, there is a significant, but unknown, risk of poor identification result.

Several studies have shown that the reconstructed hysteresis loop can be used as a subjective, visual and quantitative indicator for damage assessment (Cifuentes and Iwan 1989; Iwan 2002; Stephens and Yao 1987). If the hysteresis loops for each floor are established in real-time from data obtained during the earthquake, the general shape of the reconstructed hysteresis loops can then be examined quickly as an indicator of different types of structural behaviour. However, this approach cannot directly identify the quantitative damage severity.

Recently, a two-step regression analysis algorithm was conducted on the reconstructed hysteresis loop of a base isolated structure to identify the initial stiffness, hardening stiffness and viscous damping of the system (Xu et al. 2014). However, this regression analysis cannot be implemented automatically and cannot be applied to highly nonlinear structures with pinching behaviour. Thus, a hysteresis loop analysis method based on the hypothesis test and overall least square linear regression, was proposed for parameter identification of a SDOF pinching system using reconstructed hysteresis loops (Zhou et al. 2015). This method showed the ability to track the variation of elastic and plastic stiffness automatically if degradation occurs during the earthquake and can be readily generalized to multi degree of freedoms systems with different hysteretic behaviour.

In this study, a real-time identification algorithm is developed, based on the method presented by (Zhou et al. 2015) for seismic damage detection. The monitoring algorithm is applied to an experimental scaled reinforced concrete frame building under a shaking table test (Lu and Li 2004) to experimentally demonstrate the feasibility and robustness for highly nonlinear response. Only acceleration measurements, which can be easily obtained with low cost accelerometers and distributed over the internet in real time if necessary, were used as input information to the algorithm. Severity assessment and localization of structural damage are achieved by tracking changes in elastic story stiffness as a damage index over time, and validated against experimental measurements and observations.

2 TEST STRUCTURE

A shaking table test was conducted on a 1/10 scaled structural model of a 12-story reinforced concrete (RC) frame building, as shown in Figure 1(Lu and Li 2004). The total height of the model was 3600mm excluding a 200mm high rigid base and the model has a plan size of 600×600 mm with 12 mm thick slab for each floor. All the columns have a constant cross section 50×60 mm, and beams have same cross section of 30×60 mm. Figure 1(b) shows the elevation and main dimension of the test structure. The seismic weight of each floor for this model is 29.8 kg, including artificial mass.

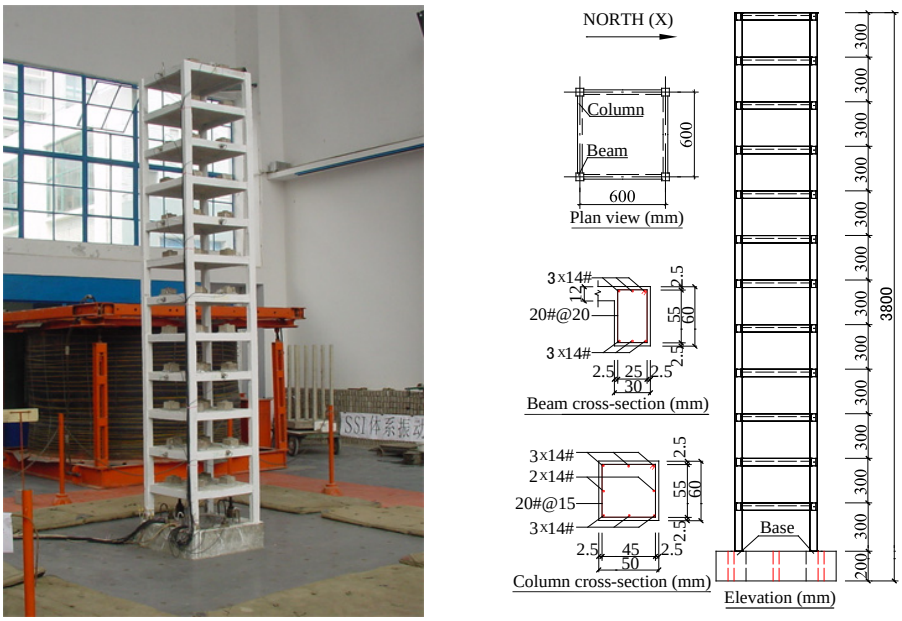

(a) **(b)**

Figure 1. (a) Photo of shaking table test of RC model, and (b) Elevation of the testing RC model.

Two stages of input acceleration based on Shanghai artificial wave (SHW) were applied in uniaxial direction (*X* direction), denoted SHW1 and SHW2. The peak ground accelerations (PGA) used in this article are scaled to 0.09g for SHW1 and 0.258g for SHW2. Figure 2 shows the time histories of the scaled input ground motions. The accelerations of the test structure were recorded in *X* direction at the base and every two levels, comprising the 2nd, 4th, 6th, 8th, 10th and 12th (top) floors.

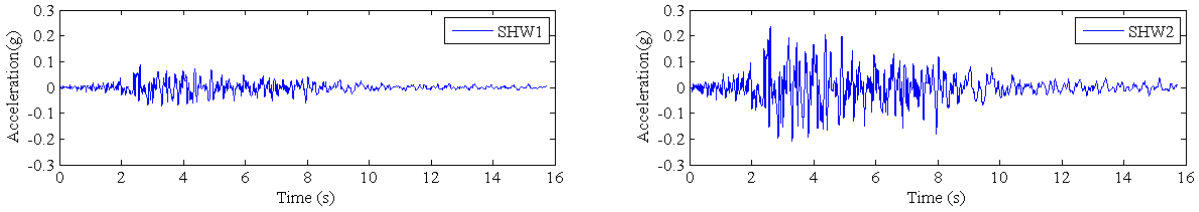

(a) **(b)**

Figure 2. Time histories of scaled testing ground motion SHW1 and SHW2.

3 RECONSTRUCTED HYSTERESIS LOOPS

To reconstruct a hysteresis loop, the measured acceleration at each DOF is required. Therefore, every two levels are approximately modelled as a single degree of freedom, and the test structure is reduced to a six degree of freedom system. The equation of motion for the inelastic system subjected to earthquake excitation can be expressed:

$$F = -\tilde{M}I\ddot{x}_g - \tilde{M}\ddot{X} - C\dot{X} \tag{1}$$

where $\tilde{M}$ is the equivalent mass matrix. The damping matrix C is approximated by assuming 5% Rayleigh damping ratio for the first and second modes since similar material and damping mechanism are distributed over the height (Chopra, 1995). The restoring force vector F is defined:

$$F_j = \begin{cases} f_j - f_{j+1} & 1 \le j \le N-1 \\ f_j & j = N \end{cases} \tag{2}$$

where f_j is the restoring force between the j^{th} and $(j\text{-}1)^{th}$ DOF. Combining Equations (1) and (2), f_j can be expressed:

$$f_j = \sum_{i=j}^{N} F_i = \sum_{i=j}^{N} (-\tilde{m}_i \ddot{x}_g - \tilde{m}_i \ddot{x}_i - [C\dot{X}]_i) \tag{3}$$

The displacements and velocities can be obtained by direct integration after band pass filtering with a cut-off frequency 0.5-30Hz. Thus, the hysteresis loops representing the structural response for the j^{th} DOF are finally reconstructed using the computed restoring force f_j and relative deformation (x_j-x_{j-1}). Figure 3 shows the reconstructed hysteresis loops for each DOF under SHW1 and SHW2. It is clear that as PGA increases, the structure goes from linear to highly nonlinear.

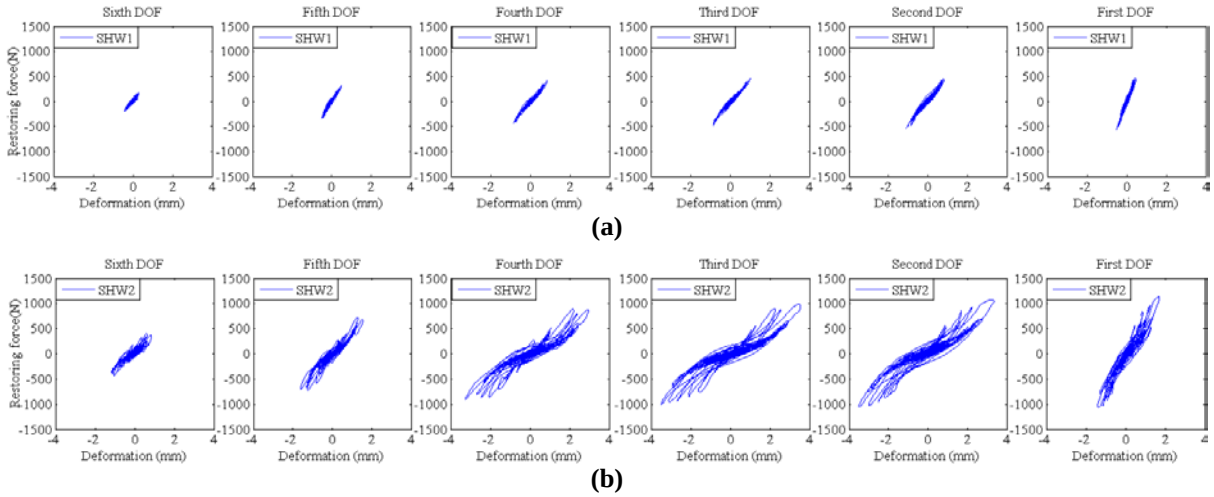

(a)

(b)

Figure 3. Reconstructed hysteresis loops for each DOF (left to right, descending to base) under (a) SHW1 and (b) SHW2.

4 HYTERESIS LOOP ANALYSIS METHOD

The evolution of the elastic story stiffness, which is used as a damage index in this algorithm, is tracked over time by calculating the slope of the elastic part of each half cycle of response. In particular, the hysteresis loop is divided into a number of half cycles in chronological order using the turning points where the deformation is a local maximum or minimum. Then the selected half cycle is first assumed to be an r-segment linear model separated by r-1 breakpoints.

Breakpoints are found by minimising the overall sum squared residual R_r:

$$R_r(\boldsymbol{\theta}) = \sum_{i=1}^{r} (G_i - a_i U_i - b_i)^2 \tag{4}$$

where G_i and U_i are the vectors of restoring force and relative displacement in the i^{th} segment (T_i), a_i and b_i are the regression coefficients in the i^{th} segment, and $\boldsymbol{\theta}$=[X_1, X_2, …, X_{r-1}] is the breakpoints vector for an r-segment model.

Using the identified breakpoints (X_1, X_2, …, X_{r-1}), the half cycles is divided into r-segments, T_1, T_2,…, T_r. An additional breakpoint is then applied to this half cycle with the identified breakpoints fixed. Thus, the half cycle is now assumed as an r+1 segment model, and the overall residual sum of squares R'_{r+1} for this model fitting is given by:

$$R'_{r+1} = \min_{1 \le j \le r} \inf_{X_r \in \Lambda_{i,\eta}} R_{r+1}(X_1, ..., X_{j-1}, X_r, X_j, ..., X_{r-1}) \tag{5}$$

$$\Lambda i, \eta = \{X_r ; X_{j-1} + 0.05(X_j - X_{j-1}) \le X_r \le X_{j-1} - 0.05(X_j - X_{j-1})\} \tag{6}$$

The F type test is used to identify the segment number of the selected half cycle and defined:

$$F(r+1|r) = n(\sum_{i=1}^{r} R_1(T_i) - R'_{r+1}) / R_r \quad (7)$$

If the value of $F(r+1|r)$ is larger than a predefined critical value, the input half cycle is identified as an $r+1$ segment. Otherwise, the new assumption of an r-1 segment model is used, and the identification procedure is reiterated.

It is noted that the stiffness degradation and damage of a structure are mainly caused by yielding deformation (Powell and Allahabadi 1988) and cracking of concrete (Basu 2005) with pinching behaviour observed in the reconstructed hysteresis loop. Thus, the stiffness in the elastic half cycles with small deformations are not considered to be different from the half cycle before, and only the half cycles with deformation more than a threshold value are used for stiffness calculation in the algorithm. The threshold value is defined as 0.6% of the story height, because limit data suggest that the yielding displacement of a building, deformed in a pattern similar to the fundamental mode, is often 0.6~0.9% of the building height (Black and Aschheim 2000). In addition, the large deformation half cycles selected using this threshold provide a larger and more adequate sample size for the statistical analysis, and thus ensure a statistically significant decision and will also better estimate the regression coefficients (Brooks and Barcikowski 2012).

Therefore, the number of segments assumed by the algorithm starts from r=3 to identify if the input half cycle has a hysteresis loop with 4-segments, representing a half cycle with both yielding and pinching behaviour. Then r=2 is applied to identify any 3-segment half cycles with pinching behaviour. Once the number of segments of the selected half cycle is identified, standard linear regression is implemented to the elastic part of the half cycle, and the elastic story stiffness in this half cycle is estimated using the slope value of this elastic part. The method is presented in full detail in Zhou et al. (2015).

5 MONITORING RESULTS OF TEST STRUCTURE

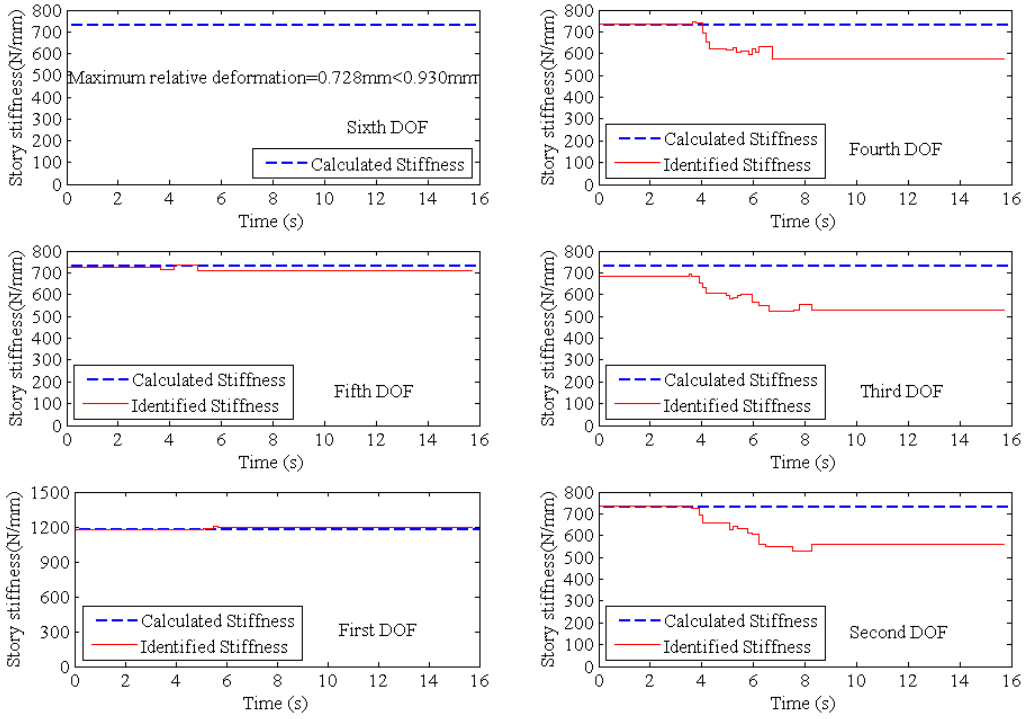

Figure 4. Evolution of story stiffness of each DOF under SHW1.

Figure 4 shows the identified evolution of elastic story stiffness of each DOF under the SHW1 input ground motion. The scaling of the elastic modulus for the model material is 1/3.87, and the story height for each DOF is 600mm. Thus, the threshold value is calculated using 0.6% of the story height by considering the scaling theory (Harris and Sabnis, 1999). It can been seen that the maximum deformation for the sixth DOF is 0.728mm, which is less than the threshold value of 0.930mm. Therefore, no half cycles are selected for stiffness calculation and stiffness degradation is not considered for the sixth DOF under SHW1. In addition, the identified initial stiffness for the other DOFs matched well with the calculated stiffness, which implies the accuracy of the algorithm on a completely linear response.

Figure 4(a) also shows no significant stiffness degradation is identified for the first, fifth and sixth DOF, which indicates these floors were behaving within a totally elastic response without damage subjected to SHW1. However, stiffness for the second, third and fourth DOF dropped 23%, 26% and 21% compared to the initial stiffness after SHW1, as shown in Figure 4(b). Visual detection was implemented, but no cracks were observed after SHW1 (Lu and Li, 2004). However, slight pinching behaviours, which are caused by opening or closing cracks of concrete, were observed from the hysteresis loops of these DOFs as shown in Figure 3(a). Thus, the structural elements of these floors could have experienced micro cracking or reinforcement slip during SHW1, though they were not significantly damaged by appearance. Hence, the method has detected what is visually clear in Figure 3(a), and quantified and localized the damage.

SHW2 is much stronger than SHW1. Therefore, significant pinching behaviours were observed from the hysteresis loops of all the DOFs, as shown in Figure 3(b). Figure 5 shows the evolution of the elastic story stiffness of each DOF during SHW2. Again, the identified initial stiffness for the first, fifth and sixth DOF matched well with the calculated stiffness, because no stiffness degradation occurred for these DOFs during SHW1. Further, significant stiffness degradation for the test structure was identified during SHW2 for all the DOFs. In particular, the stiffness for the first, fifth and sixth DOF dropped 35%, 34% and 28%, respectively, compared to the calculated stiffness. And the stiffness for the second, third and fourth DOF dropped 66%, 63% and 55% compared to the calculated stiffness.

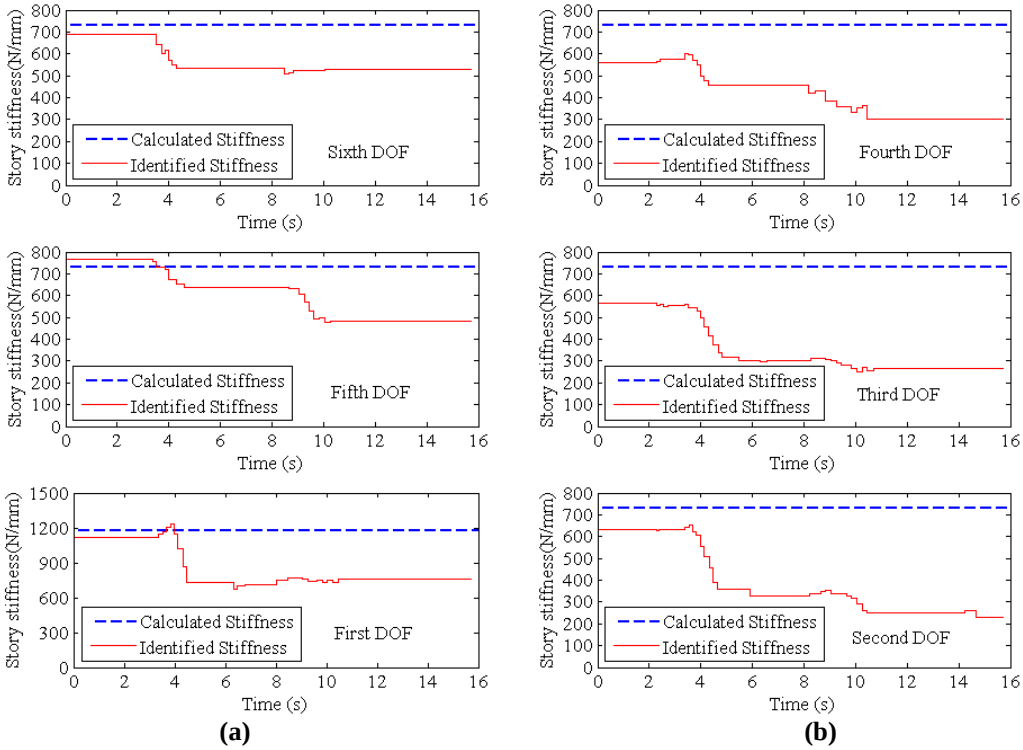

Figure 5. Evolution of story stiffness of each DOF under SHW2.

Visual detection after SHW2 showed vertical cracks were observed at the beam-column joint connection at floors 6, 5 and 4 (Lu and Li 2004), which corresponds to the large drop of stiffness of the fourth, third and second DOF. Therefore, the damage state of the test structure were successfully assessed by tracking the evolution of the elastic stiffness and a large drop of stiffness over 50% indicated significant damage occurred to the structure.

6 CONCLUSIONS

In this study, a real-time structural health monitoring algorithm was applied to a 12-story scaled reinforced concrete frame structure subject to two stages of input ground motions, SHW1 and SHW2. The test structure was assessed to be within safe stage after SHW1, because no stiffness degradation was detected for the first, fifth and sixth DOF, and less than 26% losses of stiffness were identified for the other DOFs. Significant damage was then identified during SHW2 for the second, third and fourth DOF with over 50% losses of stiffness, and visual cracks detected at the beam-column joint connection of the corresponding floors. The results show that the monitoring algorithm is capable of assessing damage severity and location by tracking the evolution of elastic stiffness of each story with only accelerations recorded.

7 ACKNOWLEDGEMENTS

The China Scholarship Council (No. 201306260119) in support of this study is greatly acknowledged. The shaking table test data used in this study was obtained from the Nature Science Foundation of China (NSFC) Project No (50338040, 50025821). The authors would like to thank Dr Peizhen Li for generously providing the experimental data.

REFERENCES

Baptista F.G., Vieira Filho J. & Inman D.J. (2012), Real-time multi-sensors measurement system with temperature effects compensation for impedance-based structural health monitoring, *Structural Health Monitoring*, 11(2), 173-186.

Basu B. (2005), Identification of stiffness degradation in structures using wavelet analysis, *Construction and building materials*, 19(9), 713-721.

Black E.F. & Aschheim M. (2000), *Seismic design and evaluation of multistory buildings using yield point spectra*, Mid-America Earthquake Center, Urbana, Ilinois.

Brooks G.P. & Barcikowski R.S. (2012), The PEAR method for sample sizes in multiple linear regression, *Multiple Linear Regression Viewpoints*, 38(2), 1-16.

Chase J.G., Leo Hwang K., Barroso L. & Mander J. (2005a), A simple LMS‐based approach to the structural health monitoring benchmark problem, *Earthquake engineering & structural dynamics*, 34(6), 575-594.

Chase J.G., Spieth H.A., Blome C.F. & Mander J. (2005b), LMS‐based structural health monitoring of a non‐linear rocking structure, *Earthquake engineering & structural dynamics*, 34(8), 909-930.

Chopra A.K. (1995), *Dynamics of structures*, Prentice Hall, New Jersey.

Cifuentes A.O. & Iwan W.D. (1989), Nonlinear system identification based on modelling of restoring force behaviour, *Soil Dynamics and Earthquake Engineering*, 8(1), 2-8.

Doebling S.W., Farrar C.R., Prime M.B. & Shevitz D.W. (1996), *Damage identification and health monitoring of structural and mechanical systems from changes in their vibration characteristics: a literature review*, Los Alamos National Lab., NM (United States), Los Alamos National Lab., NM (United States).

Harris H.G. & Sabnis G. (1999), *Structural modeling and experimental techniques*, CRC press,

Hsieh K.H., Halling M.W. & Barr P.J. (2006), Overview of vibrational structural health monitoring with representative case studies, *Journal of Bridge Engineering*, 11(6), 707-715.

Iwan W.D. (2002), *R-SHAPE: a real-time structural health and performance evaluation system*, Proceedings of the US Europe Workshop on Sensors and Smart Structures Technology, Lombardo, January.

Ko J. & Ni Y. (2005), Technology developments in structural health monitoring of large-scale bridges, *Engineering structures*, 27(12), 1715-1725.

Loh C.-H., Lin C.-Y. & Huang C.-C. (2000), Time domain identification of frames under earthquake loadings, *Journal of Engineering Mechanics*, 126(7), 693-703.

Lu X. & Li P. (2004), *Benchmark test of a 12-story reinforced concrete frame model on shaking table*, State Key Laboratory of Disaster Reduction of Civil Engineering, Shanghai, China.

Nayyerloo M., Chase J., MacRae G. & Chen X. (2011), LMS-based approach to structural health monitoring of nonlinear hysteretic structures, *Structural Health Monitoring*, 10(4), 429-444.

Powell G.H. & Allahabadi R. (1988), Seismic damage prediction by deterministic methods: concepts and procedures, *Earthquake Engineering & Structural Dynamics*, 16(5), 719-734.

Smyth A.W., Masri S.F., Kosmatopoulos E.B., Chassiakos A.G. & Caughey T.K. (2002), Development of adaptive modeling techniques for non-linear hysteretic systems, *International Journal of Non-Linear Mechanics*, 37(8), 1435-1451.

Spencer B.F., Ruiz‐Sandoval M.E. & Kurata N. (2004), Smart sensing technology: opportunities and challenges, *Structural Control and Health Monitoring*, 11(4), 349-368.

Stephens J.E. & Yao J.T. (1987), Damage assessment using response measurements, *Journal of Structural Engineering*, 113(4), 787-801.

Vafaei M., Adnan A.B. & Abd. Rahman A.B. (2013), Real-time seismic damage detection of concrete shear walls using artificial neural networks, *Journal of Earthquake Engineering*, 17(1), 137-154.

Wu M. & Smyth A. (2008), Real-time parameter estimation for degrading and pinching hysteretic models, *International Journal of Non-Linear Mechanics*, 43(9), 822-833.

Xu C., Chase J.G. & Rodgers G.W. (2014), Physical parameter identification of nonlinear base-isolated buildings using seismic response data, *Computers & Structures*, 145(1), 47-57.

Yang J.N. & Lin S. (2004), On-line identification of non-linear hysteretic structures using an adaptive tracking technique, *International Journal of Non-Linear Mechanics*, 39(9), 1481-1491.

Yao R. & Pakzad S.N. (2014), Time and frequency domain regression‐based stiffness estimation and damage identification, *Structural Control and Health Monitoring*, 21(3), 356-380.

Zhou C., Chase J.G., Rodgers G. W., Tomlinson H. & Xu C. (2015), Physical Parameter Identification of Structural Systems with Hysteretic Pinching, *Computer‐Aided Civil and Infrastructure Engineering*, 30(4), 247-262.